Schmidt, R. R., Betz, H., & Rehm, H. (1988) *Biochemistry 27*, 963-967.
Schmieden, V., Grenningloh, G., Schofield, P. R., & Betz, H. (1989) *EMBO J. 8*, 695-700.
Schmitt, B., Knaus, P., Becker, C-M., & Betz, H. (1987) *Biochemistry 26*, 805-811.
Schofield, P. R., Darlison, M. G., Fujita, N., Rodriguez, H., Burt, D. R., Stephenson, F. A., Rhee, L. M., Ramachandran, J., Glencorse, T. A., Reale, V., Seeburg, P. H., & Barnard, E. A. (1987) *Nature (London) 328*, 221-227.
Schwarz, T. L., Tempel, B. L., Papazian, D. M., Jan, Y. M., & Jan, L. Y. (1988) *Nature (London) 331*, 137-145.
Sontheimer, H., Becker, C.-M., Pritchett, D. B., Schofield, P. R., Grenningloh, G., Kettenmann, H., Betz, H., & Seeburg, P. H. (1989) *Neuron 2*, 1491-1497.
Stroud, R. M., & Finer-Moore, J. (1985) *Annu. Rev. Cell. Biol. 1*, 317-351.
Stühmer, W., Stocker, M., Sakmann, B., Seeburg, P. H., Baumann, A., Grupe, A., & Pongs, O. (1988) *FEBS Lett. 242*, 199-206.
Stühmer, W., Conti, F., Suzuki, H., Wang, X., Noda, M., Yahagi, N., Kubo, H., & Numa, S. (1989) *Nature (London) 339*, 597-603.
Südhoff, T. C., Lottspeich, F., Greengard, P., Mehl, E., & Jahn, R. (1987) *Science 238*, 1142-1144.
Tanabe, T., Takeshima, H., Mikami, A., Flockerzi, V., Takahashi, H., Kangawa, K., Kojima, M., Matsuo, H., Hirose, T., & Numa, S. (1987) *Nature (London) 328*, 313-318.
Tempel, B. L., Papazian, D. M., Schwarz, T. L., & Jan, L. N. (1987) *Science 237*, 770-775.
Tempel, B. L., Jan, Y. N., & Jan, L. Y. (1988) *Nature (London) 332*, 836-843.
Thomas, L., Hartung, K., Langosch, D., Rehm, H., Bamberg, E., Franke, W. W., & Betz, H. (1988) *Science 242*, 1050-1053.
Thomas, L., Knaus, P., & Betz, H. (1989) in *Molecular Biology of Neuroreceptors and Ion Channels* (Maelicke, A., Ed.) pp 283-289, Springer, Berlin, Heidelberg, and New York.
Timpe, L. C., & Jan, L. Y. (1987) *J. Neurosci. 7*, 1307-1317.
Timpe, L. C., Jan, J. N., & Jan, L. Y. (1988a) *Neuron 1*, 659-667.
Timpe, L. C., Schwarz, T. L., Tempel, B. L., Papazian, D. M., Jan, Y. N., & Jan, L. Y. (1988b) *Nature (London) 331*, 143-145.
Trimmer, J. S., Cooperman, S. S., Tomiko, S. A., Zhou, J., Crean, S. M., Boyle, M. B., Kallen, R. G., Sheng, Z., Barchi, R. L., Sigworth, F. J., Goodman, R. H., Agnew, W. S., & Mandel, G. (1989) *Neuron 3*, 33-49.
Unwin, N. (1986) *Nature (London) 323*, 12-13.
Unwin, P. N. T., & Zampighi, G. (1980) *Nature (London) 283*, 545-549.
Unwin, P. N. T., & Ennis, P. D. (1984) *Nature (London) 307*, 609-613.
Vassilev, P. M., Scheuer, T., & Catterall, W. A. (1988) *Science 241*, 1658-1661.
Wada, K., Ballivet, M., Boulter, J., Connolly, J., Wada, E., Deneris, E., Swanson, L. W., Heinemann, S., & Patrick, S. (1988) *Science 240*, 330-334.
Wiedenmann, B., & Franke, W. W. (1985) *Cell 41*, 1017-1028.
Ymer, S., Schofield, P. R., Draguhn, A., Werner, P., Köhler, M., & Seeburg, P. H. (1989) *EMBO J. 8*, 1665-1670.

Accelerated Publications

Evidence from X-ray Absorption Fine Structure Spectroscopy for Significant Differences in the Structure of Concanavalin A in Solution and in the Crystal†

S.-L. Lin,*,‡ E. A. Stern,‡ A. J. Kalb (Gilboa),§ and Y. Zhang‡

Department of Physics, FM-15, University of Washington, Seattle, Washington 98195, and Department of Biophysics, Weizmann Institute of Science, Rehovot, Israel

Received January 18, 1990; Revised Manuscript Received February 15, 1990

ABSTRACT: We have used X-ray absorption fine structure spectroscopy (XAFS) to study and compare the structure of concanavalin A in crystals and in aqueous solution. Significant differences were found between crystal and solution in the configuration of the transition-metal site of the protein. The metal has six ligands in solution but only five in the crystal. The ligand bond lengths are shorter in the crystal than in solution. The vibrational disorder in the crystal and possibly the corresponding bond length show a negative temperature dependence whereas in solution they vary normally with temperature. The anomalous temperature dependence in the crystal suggests that as the temperature decreases the protein molecules are subject to additional stresses, which are transmitted as a tensile stress at the metal site leading to distorted geometry and lengthening and weakening of metal-ligand bonds.

Protein structure in solution and in the crystal has not been probed with the same technique to atomic resolution. Lack of such a direct comparison sometimes leads to a presumption that there may not be consequential differences in these two states. It has been noted recently that structures of some small proteins resolved by solution 2-D NMR can differ from their X-ray crystallographic counterparts [Wuthrich et al. (1989) and references cited therein]. However, there is the possibility

† This work was funded by NSF under Grant DMB-8613948.
‡ University of Washington.
§ Weizmann Institute of Science.

0006-2960/90/0429-3599$02.50/0

that differences seen may involve the difference in the two techniques used to probe the proteins. It is therefore desirable to compare the two states by the same technique. We have done this by using the XAFS[1] technique, taking advantage of its capacity of determining local structure about a particular atom in both the crystal and solution states with higher precision than other techniques (Stern & Heald, 1983).

The protein we used in the XAFS comparison study is concanavalin A, a saccharide-binding protein from Jack bean (Summer, 1919). The protein has two distinct metal sites, one of which is normally filled with Ca and one of which is a transition-metal site that can accommodate a Zn ion. We measured as a function of temperature the structure of the first coordination shell of Zn for protein samples in both crystal and solution forms, as well as a few Zn compounds used as standards. Also studied were concanavalin A samples with Ni in the transition-metal site or with Cd replacing Ca in the other site. We report here in detail the important differences found between the two states of the protein with Zn and Ca. The results with Ni and Cd are similar and will be presented in another publication.

Materials and Methods

Concanavalin A was prepared from Jack bean meal (Sigma Chemical Co., St. Louis, MO). Solutions samples were prepared by removal of the naturally occurring metals by acid treatment and addition at pH 5.2 in 1 M NaCl of Zn, Ni, Ca, or Cd salts as required (Shoham et al., 1973). The solutions were 1 M in NaCl in order to achieve a protein concentration greater than 1 mM. The Zn protein concentration was 2 mM or more while the aqueous Zn concentration was 0.1 mM. Polycrystalline slurries were prepared as described for *I*222 crystals of concanavalin A prepared for X-ray diffraction study by equilibration of the above solutions against 0.1 M $NaNO_3$ at pH 6.5 (Greer et al., 1970). For cryogenic experiments, 40% galactose (Sigma grade crystalline, Sigma Chemical Co., St. Louis, MO) was added to the solutions and 50% 2-methyl-2,4-pentanediol to the polycrystalline slurries to inhibit formation of ice crystals at low temperatures. Ice suppression was attained by quenching the room temperature solution into liquid nitrogen. Besides minimizing the possibility of damage to the protein, ice inhibition also eliminated a noise background of Bragg peaks in the XAFS data. Solution samples without galactose were also measured at room temperature and verified that no significant effect on the XAFS occurred by its addition.

XAFS experiments were performed at the NSLS X-11 beam line. The protein samples were measured at the Zn K-edge in a fluorescence mode (Stern & Heald, 1983). Zn-Fmt (AESAR, Johnson Matthey Inc.) and other standards were prepared as powders and measured in a transmission mode. Standards and protein samples were measured at 80 and 300 K. Low temperatures were maintained with an Air Products Displex refrigerator during the measurements. Measurements of proteins at 300 K were repeated before and after 80 K measurements. No significant difference was found between the two sets of 300 K data. The small percentage of Zn atoms not incorporated in the proteins in solution (<5%) will give an error to the protein structure which is within our other uncertainties. The polycrystals that composed the slurries were fine enough so that hundreds of them were illuminated by the X-ray beam, assuring no appreciable preferred orientation effects.

The absorption data of all samples were processed by standard methods to obtain the normalized XAFS spectra χ of the first shell (Stern & Heald, 1983). Comparisons of the spectra were taken between different temperatures of the same samples and between different samples at the same temperatures by use of

$$\frac{A_1}{A_2} = \frac{N_1}{N_2}\frac{R_2^2}{R_1^2}\exp(-2k^2\Delta\sigma^2) \quad (1)$$

$$\phi_1 - \phi_2 = 2k\Delta R \quad (2)$$

where A_1 and A_2 are the amplitudes and ϕ_1 and ϕ_2 the phases of the two spectra, respectively, N_1 and N_2 are the coordination numbers of the Zn ion, R_1 and R_2 are the average ligand bond lengths, ΔR is their difference, and $\Delta\sigma^2$ is the difference in the mean squared disorder in the bond lengths of the two species. the wavenumber k of the K-shell excited photoelectron is given in reciprocal angstroms by $k^2 = 0.263(E - E_0)$, where E is the X-ray energy and E_0 is the core binding energy, both in electronvolts.

Zn-Fmt has six oxygens surrounding the Zn atom at an average distance of 2.11 Å, with a mean square structural variation of 0.0015 Å^2 (Burger & Fuess, 1976). This value was taken into account when $\Delta\sigma^2$ was calculated between a protein sample and Zn-Fmt. A correction of 0.0012 Å^2 was also added to account for the difference between measurements by the fluorescence and transmission modes (Stern & Heald, 1983). The uncertainties shown in the table and the figures were assessed from both the experimental noise and the variations introduced by data analysis. In isolating the first coordination shell of atoms for analysis, a correlation is introduced between k space points. The consequence is that only points separated by a finite k range are independent (Lee et al., 1981). This factor is accounted for in the estimation of the uncertainties and in the plot of Figure 3.

A simple Einstein model was employed to fit the vibrational amplitude data of a Zn–O bond versus temperature (Stern & Heald, 1983):

$$\sigma^2 = \frac{\hbar}{M\omega}\left[\frac{1}{\exp(\hbar\omega/k_BT) - 1} + \frac{1}{2}\right] \quad (3)$$

where $M = M_1M_2/(M_1 + M_2)$ is the reduced mass for the pair of Zn of mass M_1 and O of mass M_2. σ^2 is the mean squared vibrational disorder of bond length at temperature T, and ω is the Einstein frequency. The force constant corresponding to this harmonic oscillator can then be calculated by $M\omega^2$. An all-oxygen configuration was assumed for the first shell of the species being modeled. An insignificant error is introduced by this assumption for concanavalin A which has only one nitrogen mixed in, with the oxygen (Hardman et al., 1982).

Results

Figure 1 shows a $k^3\chi(k)$ comparison of the protein crystal, its solution, and the standard Zn-Fmt at 80 K. The qualitative differences between the two forms of the protein are clearly seen in the XAFS signal in their amplitude and phase (see Figure 1a) and in the near-edge absorbance (see Figure 1b). Their Fourier-transform magnitudes in r space are shown in Figure 2. The differences in the first shell are apparent in the first peak of the two curves, and the better order in solution is apparent by the larger amplitude peak at 3.7 Å.

The Zn-Fmt spectrum is closely similar to those of the protein samples, in both the near-edge and extended regions (see Figure 1), indicating Zn-Fmt can be used as a good

[1] Abbreviations: XAFS, X-ray absorption fine structure spectroscopy; NSLS, national synchrotron light source at Brookhaven National Laboratory; Zn-Fmt, zinc formate dihydrate [$Zn(HCOO)_2{\cdot}2H_2O$]; $\hbar$, Planck's constant; k_B, Boltzmann's constant.

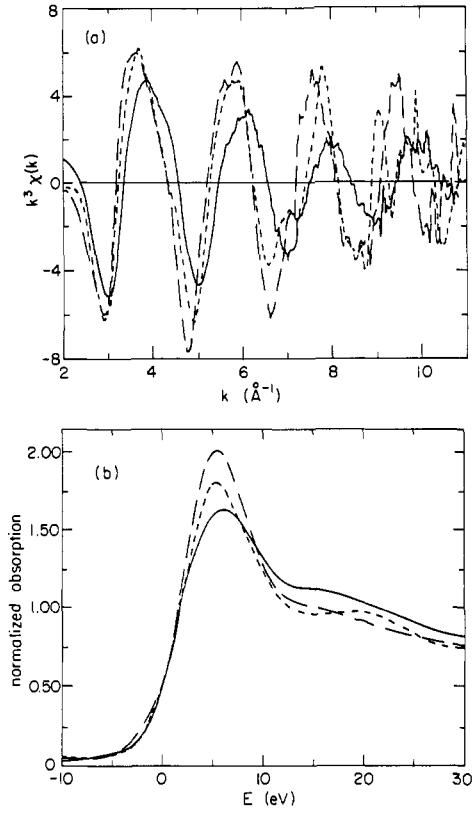

FIGURE 1: (a) Normalized Zn K-edge XAFS spectra $k^3\chi(k)$ as a function of k for Zn,Ca concanavalin A in the crystal (solid) and solution (long dash) and for Zn-Fmt (short dash) at 80 K. (b) Near-edge absorption plotted against energy, for the same samples as in (a). The data are all normalized to an edge step of $\Delta\mu x = 1$.

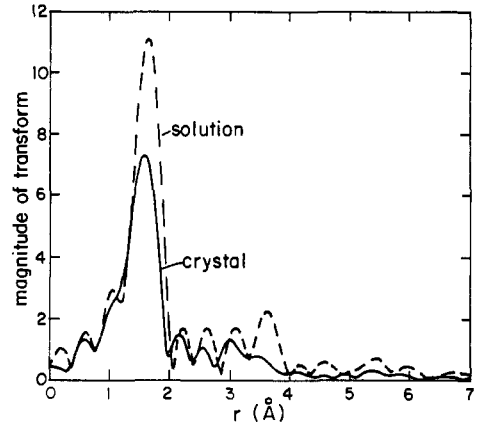

FIGURE 2: r space magnitude of transform of $k^3\chi(k)$ over the range $2 < k < 10$ Å^{-1}, for concanavalin A in the crystal (solid) and solution (dash) at 80 K.

standard in the analysis. This is verified in the sample–standard comparisons, by the linearity of the plots (see Figure 3) and the small-edge energy shifts required in the comparison, which were a fraction of an electronvolt.

The results of the comparisons are presented in Table I. The important points can be summarized as follows:

(1) At both 80 and 300 K the Zn ion in the protein has one more ligand and a longer average bond length in solution than in its crystal.

(2) There is a normal increase of vibrational disorder of the Zn site of the protein solution when the temperature rises from 80 to 300 K, while no significant change occurs in the coordination number and bond length.

(3) However, the protein crystal displays an anomalous temperature dependence. The disorder at the Zn site *decreases* with rising temperature, accompanied by a possible *shortening* of the average ligand bond length.

(4) Normal temperature behavior is also displayed at the Zn site of Zn-Fmt. Disorder increases with rising temperature, while the coordination number and ligand bond length do not change significantly.

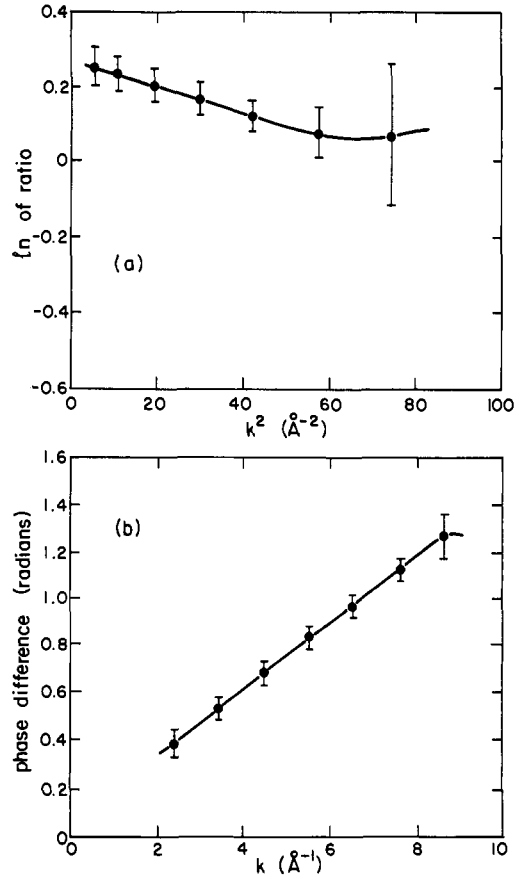

FIGURE 3: (a) Plot of the logarithm of the amplitude ratio versus k^2 and (b) plot of the difference of phase against k for concanavalin A solution versus the crystal at 300 K. The plots are for the first coordination shell about the Zn site, and the points are the independent ones. Error bars include both systematic and random uncertainties.

Table I: Structural Changes in Concanavalin A Protein and a Zn-Fmt Standard As Determined by XAFS[a]

	N_1/N_2	$\Delta\sigma^2$ (Å^2 × 10^{-3})	ΔR (Å)
soln vs cryst, 300 K	1.36 (10)	1.6 (7)	0.078 (6)
soln vs cryst, 80 K	1.30 (10)	−5.2 (7)	0.072 (6)
soln, 300 vs 80 K	0.93 (5)	5.8 (5)	0.002 (6)
cryst, 300 vs 80 K	0.96 (5)	−1.0 (5)	−0.004 (6)
Zn-Fmt, 300 vs 80 K	0.96 (5)	2.8 (5)	0.001 (6)
cryst vs Zn-Fmt, 80 K	0.84 (5)	6.6 (5)	−0.054 (6)
soln vs Zn-Fmt, 80 K	1.09 (10)	1.4 (7)	0.018 (6)

[a] $\Delta\sigma^2$ is the difference in the mean squared disorder, ΔR is the difference in average bond length, and N_1/N_2 is the ratio of the coordination number. Soln and cryst refer to concanavalin A.

Discussion

The Zn site of concanavalin A lies ~10 Å under the surface (Becker et al., 1975; Hardman et al., 1982). It is not generally recognized that crystallization can affect a structure embedded in the protein at this depth. However, the Zn site structure clearly alters from solution to the crystal. In particular, the difference in their coordination numbers is far beyond uncertainty, indicating a change of one ligand. This change is evident in the XAFS signal of the two types (Figure 1). By comparing with standards (Table I), we determine that the

Zn site in solution is hexacoordinate while in the crystal it is pentacoordinate. The average Zn–ligand bond length is larger by 0.08 Å in solution than that in the crystal. Bond length differences of this amount are expected between hexacoordinate and pentacoordinate Zn compounds. As an example, a five-coordinated compound [Zn(acetylacetone)$_2$(H_2O)] has a 2.02-Å bond, shorter by 0.09 Å than the 2.11-Å bond of the six-coordinated Zn-Fmt (Wyckoff, 1963), similar to the difference found here between the protein crystal and solution. The close similarity between Zn-Fmt and the protein suggests that the Zn site in the protein is liganded mostly with oxygens. This suggestion was investigated more quantitatively by a fitting routine using oxygen and nitrogen back-scattering amplitudes and phases obtained from formate and histidine standard compounds, respectively. The best fit occurred for one nitrogen nearest neighbor with an uncertainty of one nitrogen, verifying the predominance of oxygen neighbors.

The concanavalin A crystal also differs from its solution state in its thermal behavior (Table I). When temperature rises from 80 K to room temperature, the Zn site disorder in the protein solution increases. On the contrary, the protein crystal shows a negative temperature dependence. The Zn site becomes *more ordered* on heating, and the average Zn–ligand bond length appears to *shorten*, though this change is within uncertainty. The behavior of the solution is normal and comparable to that of Zn-Fmt. Zn-Fmt has a disorder increase, which is smaller than that in protein solution, in agreement with its shorter Zn–ligand length and hence stiffer bond (Table I). We do not have the sensitivity to detect bond changes expected from normal thermal expansion, as in Zn-Fmt and the protein solution.

It is impossible to model the protein crystal by an Einstein or any harmonic oscillator model, because of its anomalous negative temperature dependence. There is no experimental evidence for any detectable static disorder changes in the crystal with temperature. A structural disorder increase due to freezing was not observed in the solution where the protein is more exposed. Sample damage is excluded by the null effect in cycling the temperature. Conformational substates are believed to exist in proteins due to molecular flexibility, increasing static contributions to some phenomena (Frauenfelder et al., 1988). However, x-ray absorption occurs at the time scale of 10^{-15} s, much more rapid than any conformational change time scale, even at room temperature (Austin et al., 1975); i.e., the conformations are effectively frozen during an XAFS measurement, even at room temperature. In addition, a protein in solution has less constraints than a crystallized one and could be expected to suffer as much if not more static changes due to conformations. Since the solution exhibits no anomalous behavior, the conformations cannot explain the anomalous crystal behavior.

Extreme anharmonic models can be devised that give a reversed temperature dependence. One such model was proposed which invoked atoms rattling within local cavities (Gavish, 1981). At low temperatures an atom is trapped at sites offset at the extreme of the cavity. At high temperatures the atom is thermally excited to rattle around throughout the whole cavity, decreasing its σ^2 about the center. The precision of XAFS allows us to identify such a mechanism if it exists by the large zero point disorder it would predict. The normal Zn–O distance in the crystallized protein and its solution, the small value of $\Delta\sigma^2$ of the crystal relative to that of Zn-Fmt and the solution at 300 K, and the normal harmonic behavior of both Zn-Fmt and the protein in solution all preclude the existence of a cavity or any anharmonicity which imposes a large zero point disorder at the Zn site.

The anomalous temperature dependence of disorder in the crystal can be explained by the assumption of an increasing tensile stress at the Zn site as the crystal is cooled. The stress lengthens and concomitantly softens the Zn–ligand bonds, thus *increasing* the thermal disorder to an extent that more than balances the normal decreasing disorder with cooling. In a formal sense, one could equally well postulate compression of the site as the sample is warmed from 80 K to room temperature, but it seems more reasonable to assume that the site is minimally stressed under conditions wherein the protein crystallizes, namely, at room temperature, and that stress (in this case tensile stress) increases as the temperature deviates from the initial condition. Since there is no significant bond distance change with cooling, this explanation requires changes in $\Delta\sigma^2 > 10^{-3}$ Å^2 for changes in ΔR within one or two uncertainties, i.e., $\Delta R/R \approx 0.5\%$. Experiments on a variety of materials under pressure find $\Delta\sigma^2$ variations ranging from 0.3 $\times 10^{-3}$ 1.5 $\times 10^{-3}$ Å^2, for $\Delta R/R = 0.5\%$, the order of the effect needed to explain our results in the protein (Freund et al., 1989; Freund, private communication).

In a crystalline lattice a protein molecule is subject to constraints not imposed when it is in solution. Certain intermolecular geometry must be established to support protein–protein interaction. However, thermal expansion will tend to cause distortions in the molecular interface because proteins are inherently very heterogeneous. The covalent bonds along the peptide chain, the hydrogen bonds essential to secondary structure, and the van de Waals and hydrophobic interactions which prevail in higher order structures constitute a hierarchy of forces that have a very anisotropic response to thermal perturbations. As a result, the induced strain will not be evenly distributed. In particular, the segments of secondary structure which host the Zn site in concanavalin A (Becker et al., 1975; Hardman et al., 1982) will tend to slide against each other under thermal deformation, while the much stronger Zn–ligand linkages will become the focus of stress. Our experiment shows that in solution the molecules are free to adjust and relax from strain, allowing normal thermal behavior.

We have shown that a crystalline protein differs from its solution in coordination configuration and in thermal properties. The distinctive change in metal site configuration is striking considering the active role of metals in biology. Our results suggest caution in assuming that protein structure as determined from crystals will always be applicable to physiological conditions. Direct comparison techniques, such as XAFS, will be of particular importance to establish the generality of the variations in structure found here and to correctly understand the relationship between protein structure and function.

Acknowledgments

We profited greatly from comments by Professors William Parson and Ronald Stenkamp. We are grateful to P. Livins, Z. Zhang, M. Qian, D. Welch, and M. Newville as well as the NSLS X-11 staff crew for their assistance in the experiments. The NSLS facility is supported under DOE Contract DE-AC0276CH00016.

References

Austin, R. H., Beeson, K. W., Einsenstein, L., Frauenfelder, H., & Gunsalus, I. C. (1975) *Biochemistry 14*, 5355–5373.

Becker, J. W., Reeke, B. N., Jr., Wang, J. L., Cunningham, R. A., & Edelman, G. M. (1975) *J. Biol. Chem. 250*, 1513–1524.

Burger, N., & Fuess, H. (1977) *Z. Kristallogr. 145*, 346-355.
Frauenfelder, H., Parak, F., & Young, R. D. (1988) *Annu. Rev. Biophys. Biophys. Chem. 17*, 451-479.
Freund, J., Ingalls, R., & Crozier, E. D. (1989) *Phys. Rev. B 39*, 12537-12547.
Gavish, B. (1981) *Proc. Natl. Acad. Sci. U.S.A. 78*, 6868-6872.
Greer, J., Kaufman, H. W., & Kalb, A. J. (1970) *J. Mol. Biol. 48*, 365-366.
Hardman, K. D., Agarwal, R. C., & Freiser, M. J. (1982) *J. Mol. Biol. 157*, 69-86.
Lee, P. A., Citrin, P. H., Eisenberg, P., & Kincaid, B. M. (1981) *Rev. Mod. Phys. 58*, 769.
Shoham, M., Kalb, A. J., & Pecht, I. (1973) *Biochemistry 12*, 1914-1917.
Stern, E. A., & Heald, S. M. (1983) *Handbook on Synchrotron Radiation* (Koch, E. E., Ed.) Vol. 1, pp 955-1014, North-Holland Publishing Co., Amsterdam.
Summer, J. B. (1919) *J. Biol. Chem. 37*, 137-143.
Wuthrich, K. (1989) *Acc. Chem. Res. 22*, 36-44.
Wyckoff, W. G. (1965) *Crystal Structures*, 2nd ed., Wiley, New York.

Articles

Mechanism of HIV Reverse Transcriptase: Enzyme–Primer Interaction As Revealed through Studies of a dNTP Analogue, 3′-Azido-dTTP†

Padmini S. Kedar,‡ John Abbotts,‡ Terêz Kovâcs,§ Krystyna Lesiak,§ Paul Torrence,§ and Samuel H. Wilson*,‡
Laboratory of Biochemistry, National Cancer Institute, and Laboratory of Analytical Chemistry, National Institute of Diabetes and Digestive and Kidney Diseases, National Institutes of Health, Bethesda, Maryland 20892
Received August 31, 1989; Revised Manuscript Received December 26, 1989

ABSTRACT: Primer and dNTP recognition by purified HIV reverse transcriptase have been investigated. Earlier kinetic studies suggested that the reaction pathway for DNA synthesis is ordered, with template-primer and free enzyme combining to form the first complex in the reaction sequence [Majumdar et al. (1988) *J. Biol. Chem. 263*, 15657-15665], and through use of a particularly high affinity template-primer analogue [$r(I)_n$·$Sd(C)_{28}$], rate values for formation of the first complex were calculated [Majumdar et al. (1989) *Biochemistry 28*, 1340-1346]. We now report rate values for first complex formation in the usual model replication system with poly[r(A)]·oligo [d(T)] as template-primer. We find that 3′-azido-dTTP (AZTTP) is a linear competitive inhibitor of DNA synthesis against the substrate dNTP (dTTP) in the poly[r-(A)]·oligo[d(T)] replication system. This suggests that 3′-azido-dTTP and dTTP combine with the same form of the enzyme in the reaction scheme, i.e., the enzyme–primer complex. This is not trivial, since a second analogue, 3′-amino-dTTP, also is an inhibitor against dTTP, but the mechanism in this case is linear noncompetitive. Because the inhibition by 3′-azido-dTTP is linear competitive, the K_D for physical binding to the enzyme is assumed to be the same as the K_i for inhibition (20 nM). Substrate kinetic studies of DNA synthesis using 3′-azido-dTTP as substrate revealed that the Michaelis constant is 3 μM. Therefore, the K_m for this substrate analogue is 100-fold higher than the K_D for binding of the analogue to the enzyme–primer complex. This difference is consistent with the proposed kinetic scheme and is due primarily to the effect of enzyme–primer complex dissociation on the value of K_m. The results enable calculation of rate values for the enzyme–poly[r(A)]·oligo[d(T)] association (k_{on} = 2.6 × 10^8 M^{-1} s^{-1}) and dissociation (k_{off} = 39 s^{-1}) and a K_D value for dTTP binding (~180 nM).

The HIV[1] reverse transcriptase catalyzes both RNA-directed DNA synthesis and DNA-directed DNA synthesis in the cytoplasm shortly after retrovirus infection of a cell. In the first step of this process, the enzyme is capable of recognizing its natural primer, Lys-tRNA subspecies 3. The enzyme then conducts the DNA synthesis, template switching, and RNase H steps necessary for replication of the complete viral genome (Gilboa et al., 1979). The enzymatic mechanism of these events is the subject of current investigation.

As a means of understanding the mechanism of the HIV reverse transcriptase, Majumdar et al. (1988, 1989) applied steady-state kinetic and processivity analysis to obtain a kinetic scheme for the overall DNA synthetic reaction. The data suggested that the free enzyme interacts with the template-primer substrate in the initial phase of the DNA synthesis

†Supported in part by the NIH Intramural AIDS Targeted Antiviral Program.
*Address correspondence to this author.
‡National Cancer Institute.
§National Institute of Diabetes and Digestive and Kidney Diseases.

[1] Abbreviations: AZT, 3′-azido-3′-deoxythymidine; AZTTP or 3′-azido-dTTP, 3′-azido-3′-deoxythymidine 5′-triphosphate; NH_2T, 3′-amino-3′-deoxythymidine; NH_2TTP or 3′-amino-dTTP, 3′-amino-3′-deoxythymidine 5′-triphosphate; DTT, dithiothreitol; dNMP, deoxynucleoside monophosphate; dNTP, deoxynucleoside triphosphate; ddTTP, 2′,3′-dideoxythymidine 5′-triphosphate; HIV-1, human immunodeficiency virus, type 1; oligo[d(T)], oligomer of deoxythymidylate; poly[r(A)], polyriboadenylate; RT, reverse transcriptase; $Sd(C)_{28}$, 28-residue oligodeoxycytidylate with sulfur substituted at a nonbridge oxygen of each phosphate atom; T-P, template-primer; TEAB, triethylammonium bicarbonate. Polynucleotide subscripts indicate precise chain length unless otherwise noted. The kinetic nomenclature and constants are according to Cleland (1963a,b) and Fersht (1985).